Petroleum Science 21 (2024) 4391–4404

Contents lists available at ScienceDirect

Petroleum Science

journal homepage: www.keaipublishing.com/en/journals/petroleum-science

Original Paper

Synergistic effect of nanoparticles and viscoelastic surfactants to improve properties of drilling fluids

Yurany Villada [a], Lady Johana Giraldo [a], Carlos Cardona [a], Diana Estenoz [b], Gustavo Rosero [c], Betiana Lerner [d, e], Maximiliano S. Pérez [d, e], Masoud Riazi [f], Camilo A. Franco [a], Farid B. Córtes [a, *]

[a] Grupo de Investigación Fenómenos de Superficie Michael Polanyi, Departamento de Procesos y Energía, Facultad de Minas, Universidad Nacional de Colombia, Sede Medellín, 050034, Medellín, Colombia
[b] INTEC (Universidad Nacional del Litoral – CONICET), Güemes 3450, 3000, Santa Fe, Argentina
[c] Centro IREN, Universidad Tecnológica Nacional (UTN), Buenos Aires, 1706, Argentina
[d] Facultad Regional Haedo, Universidad Tecnológica Nacional (UTN), Haedo, Buenos Aires, 1706, Argentina
[e] Department of Electrical and Computer Engineering, Florida International University, Miami, FL, 33174, USA
[f] School of Mining and Geosciences, Nazarbayev University, Astana, Kazakhstan

ARTICLE INFO

Article history:
Received 12 September 2023
Received in revised form
19 September 2024
Accepted 20 November 2024
Available online 21 November 2024

Edited by Jia-Jia Fei and Teng Zhu

Keywords:
Micromodel
Nanofluids
Silica nanoparticles
Viscoelastic surfactants
Water-based drilling fluids

ABSTRACT

The conservation of rheological and filtration properties of drilling fluids is essential during drilling operations. However, high-pressure and high-temperature conditions may affect drilling fluid additives, leading to their degradation and reduced performance during operation. Hence, the main objective of this study is to formulate and evaluate a viscoelastic surfactant (VES) to design water-based drilling nanofluids (DNF). Silica nanomaterials are also incorporated into fluids to improve their main functional characteristics under harsh conditions. The investigation included: i) synthesis and characterization of VES through zeta potential, thermogravimetric analysis (TGA), Fourier transform infrared spectroscopy (FTIR), atomic force microscopy (AFM), and rheological behavior; ii) the effect of the presence of VES combined with silica nanoparticles on the rheological, filtration, thermal, and structural properties by steady and dynamic shear rheological, filter press, thermal aging assays, and SEM (SEM) assays, respectively; and iii) evaluation of filtration properties at the pore scale through a microfluidic approach. The rheological results showed that water-based muds (WBMs) in the presence of VES exhibited shear-thinning and viscoelastic behavior slightly higher than that of WBMs with xanthan gum (XGD). Furthermore, the filtration and thermal properties of the drilling fluid improved in the presence of VES and silica nanoparticles at 0.1 wt%. Compared to the WBMs based on XGD, the 30-min filtrate volume for DNF was reduced by 75%. Moreover, the Herschel-Bulkley model was employed to represent the rheological behavior of fluids with an R^2 of approximately 0.99. According to SEM, laminar and spherical microstructures were observed for the WBMs based on VES and XGD, respectively. A uniform distribution of the nanoparticles was observed in the WBMs. The results obtained from microfluidic experiments indicated low dynamic filtration for fluids containing VES and silica nanoparticles. Specifically, the filtrate volume of fluids containing VES and VES with silica nanoparticles at 281 min was 0.35 and 0.04 mL, respectively. The differences in the rheological, filtration, thermal, and structural results were mainly associated with the morphological structure of VES or XGD and surface interactions with other WBMs additives.

1. Introduction

Drilling mud accounts for approximately 15%–18% of the total costs during drilling operations. The functional properties of the drilling fluid are primarily related to the composition, rock formation properties, and operational conditions during drilling.

* Corresponding author.
E-mail address: fbcortes@unal.edu.co (F.B. Córtes).

https://doi.org/10.1016/j.petsci.2024.11.014

Drilling fluids can be categorized as water-based (WBM) or oil-based drilling fluids (OBM). Although several researchers have indicated that oil drilling muds exhibit superior performance to WBM (Alsaba et al., 2020), environmental regulations have limited the use of OBMs owing to the contents of toxic materials and problems with waste management. Therefore, the drilling industry is concentrating on developing environmentally friendly WBMs with a performance similar to that of OBM, particularly for low-permeability formations and high-temperature conditions (Aftab et al., 2020; Rana et al., 2020).

Several materials have been incorporated into designed WBMs to improve their performance. Synthetic and natural polymers (Ali et al., 2022, 2024b; Gautam et al., 2022; Karakosta et al., 2021) are the most common materials used to improve the rheological and filtration properties and to avoid formation instability issues (Ali et al., 2024a; Tahr et al., 2022, 2023). Based on their molecular properties, they fulfill specific functions such as thickeners/viscosifiers, fluid loss reducers, shale encapsulants (Saleh, 2022a), lubricants, inhibitors (Nur and Saleh, 2022), and flocculants (Caenn and Chillingar, 1996; Saleh et al., 2022). However, the thermal stability of these polymers is a significant issue at high depths and high temperatures (Al-Yasiri et al., 2019). Likewise, the viscosity of polymers is affected at high salinity and high shear rates.

According to their thickening properties generated with water and bentonite, the polysaccharides such as Arabic (Olatunde et al., 2012), locust bean (Hall et al., 2018), guar (Anderson and Baker, 1974), diutan (Ezell et al., 2010), welan (Gao, 2015), xanthan (Villada et al., 2021), and tamarind gums (Mahto and Sharma, 2004), scleroglucan (Hamed and Belhadri, 2009), chitin (Li et al., 2018a), cellulose and chitosan derivatives (Li et al., 2020a) have been widely researched as viscosifiers or filtration control agent in WMBs (Li et al., 2020b). On the other hand, starch (Carico and Bagshaw, 1978; Dias et al., 2015; Mahto and Sharma, 2004), and cellulose derivatives have been employed mainly as additives for filtrate control (Kafashi et al., 2017; Khamehchi et al., 2016). Particularly, xanthan gum has been employed as a conventional polymeric additive in WBMs. XGD produces a thixotropic and pseudoplastic fluid behavior, which enhances the filtration properties and contributes to wellbore cleaning (Ezell et al., 2010), but at high temperatures, it exhibits thermal degradation.

Owing to current advances in nanotechnology, the implementation of nanoparticles in drilling operations has been an encouraging alternative (Clavijo et al., 2021a; Rafati et al., 2018). Several nanoparticles such as silica, copper oxide, zinc oxide, aluminum oxide, graphene oxide, iron oxide, nanographite, tin oxide, carbon nanotubes, and composite nanoparticles have been studied (Agista et al., 2018; Blkoor et al., 2023; Oseh et al., 2023). Considering previous studies (Abdullah et al., 2022; Saleh, 2022b; Villada et al., 2022), incorporating nanomaterials enhances the properties of WBMs, increases the reservoir stability, and inhibits clay swelling. In particular, silica nanoparticles are one of the most used nanomaterials in WBMs owing to their exceptional properties such as surface area, controlled size, dispersibility, and surface characteristics that promote the reduction of water invasion in the formation and modification of rheology and filtration properties, among others (Fakoya and Shah, 2017). Numerous investigations have reported that silica nanomaterials significantly modify the rheological properties of WBMs (Rafati et al., 2018). Salih et al. (2016) concluded that low concentrations of silica nanomaterials improve the hydraulic, rheological, and filtration properties. Liu et al. (2016) evaluated the effect of silica nanomaterials on the efficiency of WBMs. The authors argued that nanosilica increases the transportation rate of cutting through its interaction with cuttings (Kök and Bal, 2019; Medhi et al., 2020). Clavijo et al. (2021b) experimentally and theoretically studied the interactions between silica nanoparticles and the main components of WBMs. The authors found that silica nanoparticles slightly increased the viscosity of the WBMs. In addition, lower filtrate volumes and compact and impermeable filter cakes were obtained with the addition of nanoparticles. However, Smith et al. (2018) and Li et al. (2024) concluded that high concentrations of silica nanoparticles promote nanoparticle agglomeration, leading to permeation channels, which increase fluid loss. Nanoparticle-based WBMs have been applied in the Colombian oil field (Franco et al., 2021).

The surface interactions between the components of fluids have been studied in several studies in terms of the chemical nature and physicochemical properties of the components and the continuous phase characteristics (Oseh et al., 2024). Polymer additives interact with clay through several mechanisms, such as electrostatic, hydrogen bonding, and hydrophobic interactions, and structural modifications of clay can be achieved, such as exfoliation and intercalation by additive molecules. In addition, a similar interaction mechanism was observed in the presence of a surfactant because of the complexation of the surfactant with its polar head and clay.

Viscoelastic surfactants (VES) or wormlike micelles are surfactants that exhibit viscoelastic behavior in water-based solutions. Similar to traditional surfactants, viscoelastic surfactants contain hydrophilic head groups and hydrophobic chains. Nevertheless, VES exhibits significant viscoelasticity properties associated with the formation of entangled structures and wormlike micelles owing to surface interactions in aqueous solutions (Wang et al., 2017). The formation of wormlike micelles is governed by the surfactant concentration in the solution. At low concentrations, the counterions contribute to the formation of wormlike micelle (Bao et al., 2021). At low surfactant concentrations, the solution exhibited monomolecular dispersion following Newtonian behavior. Likewise, as the concentration of the surfactant increases, micelles can expand and elongate, forming rod-like structures. Under specific entropy conditions, micelles tend to elongate and self-associate in wormlike glue (Hu et al., 2021).

VES has been used in fracturing packs, fracturing fluids, matrix acidification, and chemical flooding owing to its characteristics such as thermal and chemical stability, viscosities similar to polymers, viscoelasticity, and efficiency in oil-water interfacial tension reduction (Kang et al., 2020).

Compared with polymers, VES presents attractive advantages such as thermal and chemical stability, structural regeneration under shear stress conditions, and low solid content that avoids formation damage (Ogugbue et al., 2010). For this reason, using VES as an interesting novel alternative to conventional polymers in WBMs. Likewise, the implementation of VES with silica nanoparticles can improve the functional properties of WBMs under harsh conditions, minimize the quantities of materials required to optimize WBMs design, and reduce the operation cost. In addition, nanoparticles could contribute to the early stimulation of the well and avoid future chemical stimulation (Clavijo et al., 2021a; Smith et al., 2018).

To the best of our knowledge, publications related to the use of VES and VES combined with nanotechnology in WBM have not yet been reported. The main objective of this study was to assess the combination of VES and nanotechnology under high-temperature conditions as an alternative to improve the functional properties of WBMs. The investigation included: i) synthesis and characterization of the VES, ii) formulation of the WBMs, iii) evaluation of the effect of VES combined with silica nanoparticles on the main functional properties of the drilling fluids through steady shear rheological, filter press, thermal aging assays, and SEM, iv) a comparison of the performance of WBMs containing VES or XGD, and v) the use of a microfluidic approach to study the pore-scale mechanisms of drilling fluid filtration.

2. Materials and methods

2.1. Materials

Hexadecyltrimethylammonium bromide (CTAB; PanReac AppliChem) and sodium nitrate ($NaNO_3$; PanReac AppliChem) were used to formulate the VES. The WBMs included sodium bentonite, xanthan gum (XGD), and polyanionic cellulose (PAC) (Provided by energy sector companies). Deionized water was used to prepare the WBMs and VES. Fumed silica nanoparticles were obtained from Sigma Aldrich (United States). Table 1 summarizes the main properties reported in previous studies (Clavijo et al., 2021b).

2.2. Formulation and characterization of viscoelastic surfactants (VES)

2.2.1. VES formulation

A viscoelastic surfactant was obtained from CTAB and $NaNO_3$ (Kumar et al., 2015) in a 2:1 ratio. CTAB (5.0 g) was slowly added to 500 mL of distilled water in a single-necked flask. The solution was stirred for 30 min at 600 rpm at 25 °C. Then 2.5 g of $NaNO_3$ were slowly added to the solution, and the mixture was well stirred for 30 h at 600 rpm and 25 °C. The chemicals for the formation of VES were selected based on a previous study (Kumar et al., 2015) considering possible surface interactions.

2.2.2. Characterization of VES

Z-potential measurements were performed using Nanoplus-3 (Micromeritics, USA). Suspensions of VES at a concentration of 1 g L^{-1} were prepared in deionized water and sonicated for 10 min.

The thermal stability of the VES was determined by thermogravimetric analysis (TGA). A TA Instruments Q50 thermobalance was used. The VES sample was heated at 10 °C/min using a platinum pan from 25 up to 600 °C in a N_2 environment (80 mL/min). Each sample weighed approximately 5 mg.

The VES FTIR spectrum was obtained using an IRAffinity-1S spectrophotometer (Shimadzu, Torrance, CA, USA) in the frequency range of 4000–400 cm^{-1}. Approximately 3 mg of VES was used for analysis. Prior to the test, the VES was dried at 24 °C. KBr was used as a reference material (background spectrum).

VES AFM characterizations were conducted in the tapping mode using an Agilent 5500 (Keysight, USA) instrument. The surfaces were prepared by spin-coating on silicon wafers. Assays were performed at 2.35 Hz of amplitude velocity with a Nano World (PNP-TR-Au) triangular cantilever, using a resonance frequency of 67 kHz and force constant of 0.32 N m^{-1} and 25 °C. Measurements were performed at room temperature, and images were processed using the freeware Gwyddion software 2.49 package (SourceForge).

Steady shear analyses of VES were performed using a Kinexus Pro + rotational rheometer (Malvern Instruments, Worcestershire, UK). The cone-plate configuration was used with a shear rate range of 0.01–1000 s^{-1} at 25 °C. Prior to the measurements, the VES solutions were pre-stirred at 1000 s^{-1} for 30 s. Three replicates were performed for each measurement.

To compare the rheological properties of VES and XGD aqueous suspensions, XGD solution at 0.5 wt % (concentration commonly used in drilling formulations) was prepared. To this end, XGD was added to distilled water and stirred for 20 min at 500 rpm.

Table 1
Physicochemical properties of fumed silica nanoparticles.

Property	Value
Particle size	9.7 nm
Z potential (pH = 10)	−31.54 ± 3 mV
Surface area (SBET)	380 m^2 g^{-1}

2.3. Preparation of WBMs

To evaluate the replacement of XGD with VES and the effect of silica nanoparticles on the filtration, rheological, structural, and thermal properties of the fluids, two WBMs groups were considered: WBMs based on XGD (BT/XGD/PAC/H_2O) and WBMs based on VES (VES/BT/PAC/H_2O). Fluid preparation was conducted following the API standard (API Recommended Practice 13B-1, 2003). Likewise, WBMs containing different additives were prepared as follows: In the WBMs based on XGD, four different dosages of silica nanoparticles were employed: 0.0 (base), 0.001, 0.100, and 1.000 wt %, while PAC, XGD, and BT were fixed at 0.5, 0.5, and 1.0 wt%, respectively. In the WBM group based on VES, four concentrations of silica nanoparticles were employed: 0.000 (base), 0.001, 0.100, and 1.000 wt%, while the concentrations of PAC and BT were fixed at 0.5 and 1.0 wt%, respectively. The nomenclature of fluids indicates the type of fluid based on XGD or VES, and the content of nanoparticles ranges from 0.000 to 1.000 wt%. The detailed compositions of the fluids are presented in Table S1 (Supporting Information).

In the case of WBMs based on XGD, the following steps were performed: *i*) bentonite was hydrated for 960 min at 25 °C; *ii*) XGD was incorporated, and the mixture was stirred at 600 rpm for 10 min; *iii*) PAC was added, and the suspension was stirred for 10 min at 600 rpm. The preparation of WBMs based on VES included the following steps: *i*) 500 mL of the previously formulated VES solution was added to the vessel and stirred for 10 min; *ii*) BT was aggregated and the suspension was stirred at 600 rpm. It is important to note that VES was added as the liquid. An additional step was considered for fluids containing nanoparticles. To this end, fumed silica nanoparticles were added and the suspensions stirred at 500 rpm for 10 min.

2.4. Characterizations of WBMs

To evaluate the performance of WBMs, five assays were implemented: i) steady and dynamic shear rheology to evaluate the rheological behavior of WBMs, shear thinning behavior is recommended; ii) filtration at LTLP and HTHP to evaluate the potential loss fluid in the formation; iii) aging test to determine the thermal stability of WBMs simulating the well conditions; iv) microstructure of WBMs to understand the structure-property relationships of WBMs in the presence of nanomaterials; and v) microfluidic tests to evaluate the pore-scale mechanisms for filtration of the WBMs with and without silica nanoparticles.

Steady shear analyses of fluids were carried out using the same rheometer and conditions described for the rheological characterization of VES. To this end, 10 mL of WBMs were put on the rheometer plate, and the determinations were performed at a shear rate range of 0.01–1000 s^{-1} at 25 °C.

Oscillatory shear analyses were performed to determine the viscoelastic behavior of the WBMs. For the measurements, 10 mL of WBMs was placed on the rheometer. The assays were carried out in a Kinexus Pro + rotational rheometer (Malvern Instruments, Worcestershire, UK) coupled with a Peltier cone-plate geometry (60-mm diameter, 1° angle) at a gap of 1 mm. Frequency sweeps were conducted from 0.01 to 100 Hz within the linear viscoelastic region (LVER) at strains of 0.02, and 25 °C. To obtain the LVER an amplitude sweep from 0.01 to 0.10 at 100 Hz was performed. This assay was repeated twice.

The Herschel-Bulkley model was implemented to theoretically study the rheological behavior of the samples. The model was

adjusted using an error-minimizing routine in the complement solver of Microsoft Excel.

Filtration tests were performed according to API standards (API recommended practice 13B-1, 2003). To this end, a filter press (OFITE, Houston, TX, USA) at 25 °C and pressure of 6.80 atm was used with No. 50 Whatman filter paper. Specifically, 250 mL of WBMs was poured into a steel cell using nitrogen as pressurization gas. The filtrate was collected in a graduated cylinder for 30 min. Filter cake thickness was determined using a caliper.

The filtrate rate was calculated following the methodology reported previously (Li et al., 2024; Villada et al., 2021, 2022).

Darcy's law was employed to determine the permeability (K_c) of the filter cake of the WBMs under low-temperature and pressure conditions. The permeability is mathematically represented as (Villada et al., 2022):

$$K_c = \frac{\mu t_c q}{\Delta P A} \quad (1)$$

where μ corresponds to the viscosity of the filtrate, t_c is the filter cake thickness, ΔP is the pressure difference, A is the cross-section area and q is the filtrate rate ($cm^3\ s^{-1}$).

An HPHT filter press (Fann, Texas, USA) was employed to report the filtration volume at 30 min under pressure (34 atm) and temperature (98.8 °C). For the test, 250 mL of WBMs was poured into a steel cell using nitrogen as pressurization gas. The filtrate was collected from a steel cell. Special hardened filter paper (part number 206056) was employed.

A dynamic aging assay was conducted using a heating plate at 91 °C and 500 rpm for 960 min. WBMs (150 mL) were poured on a heating plate, and their rheological properties were obtained after the aging treatment using the methodology used previously for the VES suspensions.

The structures of the WBMs were determined using a scanning electron microscope (JEOL JSM 6490 LV, Germany). The WBMs were sputter-coated with gold (DENTON VACUUM Desk IV equipment) to ensure adequate conductivity.

2.4.1. Reologhical model

The Herschel-Buckley model (Eq. (2)) was employed to describe the rheological behavior of the WBMs.

$$\tau = \tau_0 + k\prime\gamma^{n\prime} \quad (2)$$

where τ_0 (Pa·s) is the yield stress, k' is the consistency index (mPa·s), γ (1/s) is the shear rate and n' is the flow behavior index.

2.5. Microfluidics approach

Fig. 1 shows the schematic of the microfluidic device and its experimental setup. The micromodel depth was around 99.9 μm, the pore size varies between 0.1 and 0.6 mm, porosity of 70.9 %, and the absolute permeability was 5.71 D. The micromodel was designed to simulate the pore conditions in the reservoir, achieving an injection parallel to the face of the well (or cross-flow) that allows fluid behavior in the well. A microfluidic model porous medium was fabricated using polydimethylsiloxane (PDMS). A microchannel network was fabricated with a blend of epoxy resin and a curing agent (Cristal-Tack, Novarchem, Argentina) and designed using Layout Editor Software (Germany). The details of the micromodel design have been presented in a previous study (Olmos et al., 2019).

To inject oil and drilling fluid into the micromodel, an A22-Adox Syringe Infusion pump was used at a constant flow rate to simulate reservoir conditions. The flow was recorded by capturing images with a Canon EOS T3 camera. Similarly, a backlight lamp was placed under the micromodel as an illumination source during image acquisition. To perform the test, the two micromodels were saturated with oil (API gravity of 21.9°). Then, the fluid filtration was performed at a flow rate of 1.0 ft day^{-1} (0.19 μL min^{-1}) and 25 °C.

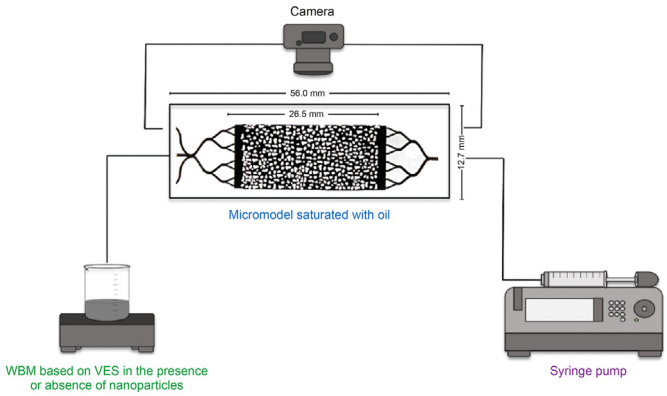

Fig. 1. Schematic of the microfluidic device and experimental setup.

3. Results and discussion

3.1. VES characterizations

Fig. 2 shows the Z potential curves for the XGD and VES solutions. VES has a negative charge (−20 mV) associated with the functional groups of CTAB and the negative charge of $NaNO_3$. Likewise, XGD shows a negative charge (−36 mV) related to the glucuronic acid of this polymer.

The TGA and DTG curves of VES are shown in Fig. 3. It was observed that VES had a high thermal stability from 25 to ~200 °C. The maximum rate of mass loss in the DTG curve was approximately 270 °C. These residues were associated with the thermal decomposition of sodium nitrate. The thermal stability of VES could be attributed to the fact that above the micellar concentration, the micellar structure is entangled and forms a network with remarkable viscoelastic properties (Gurluk et al., 2013).

The FTIR spectrum of VES is presented in Fig. 4. The asymmetric

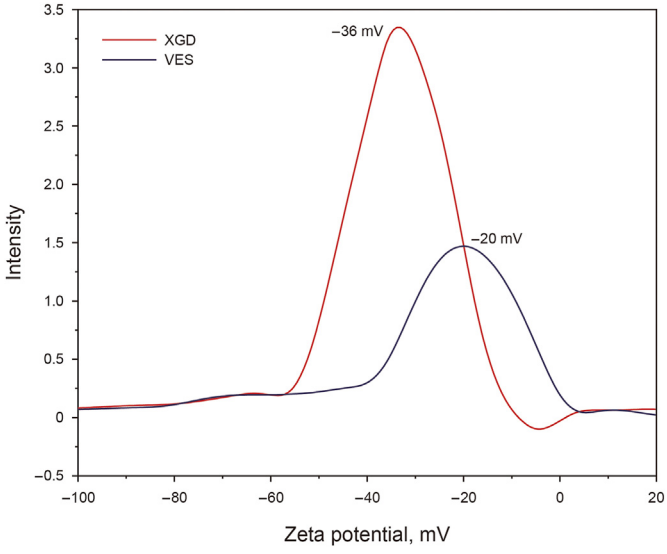

Fig. 2. Zeta potential curves for XGD and VES solutions.

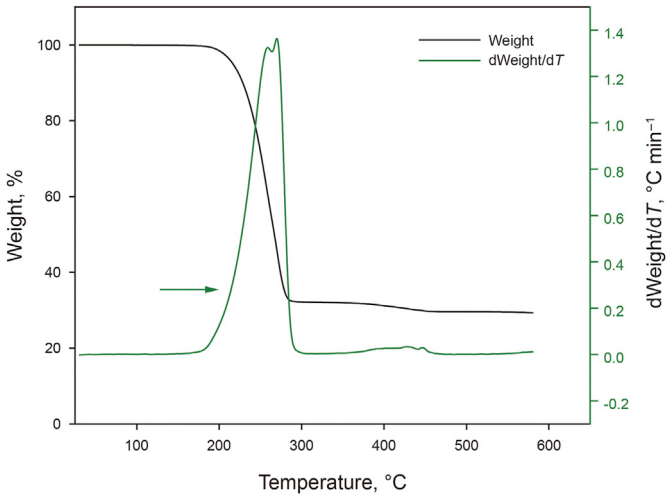

Fig. 3. Thermal stability of VES obtained from TGA and DTG analysis.

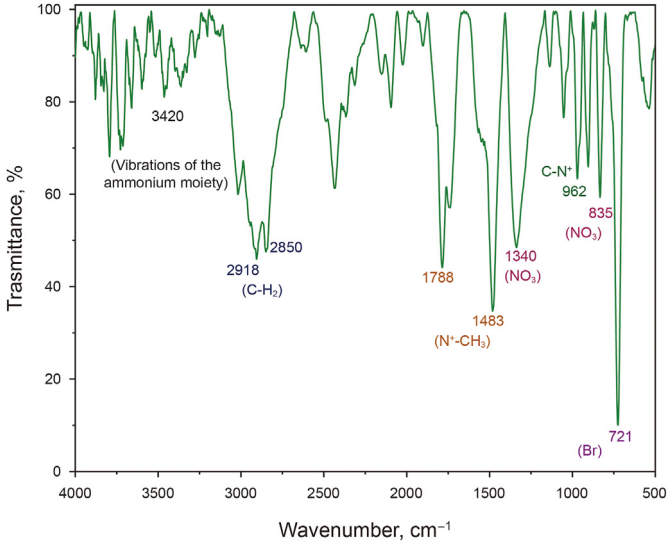

Fig. 4. FTIR spectrum of VES.

and symmetric stretching vibrations of C—CH_2 in the methylene chains can be seen in bands at 2918 and 2850 cm^{-1}, respectively. Asymmetric and symmetric stretching vibration of N^+—CH_3 are related to bands at 1788 and 1483 cm^{-1}. At 3420 cm^{-1} the vibrations of the ammonium moiety in CTAB are observed. The band at 962 cm^{-1} is related to the C—N^+ stretching vibrations. The peak at 721 cm^{-1} could be assigned to Br. The signal at 835 cm^{-1} is assigned to NO_3 symmetric stretching. The signal at 1340 cm^{-1} is associated with the NO_3 asymmetric stretching. The detected signals are in agreement with previous studies (Elfeky et al., 2017; Sui et al., 2006; Trivedi and Dahryn Trivedi, 2015; Yayapao et al., 2011).

The micelle morphology of VES was studied using AFM in the dehydrated state, as shown in Fig. 5. The AFM methodology was selected considering the nanometric scale to identify some materials, in this case, the effect of silica nanoparticles in the VES structure. AFM micrographs revealed the presence of a polydisperse structure similar to cylinders with diameters of 100–153 nm for images 5(a), (b), and (c), corresponding to topography 5(a), phase 5(b), and amplitude images 5(c). The impact of silica nanoparticles on the VES microstructure is presented in Fig. S1 (Supporting Information).

Fig. 6 compares the flow curves of the XGD and VES solutions. As expected, the presence of $NaNO_3$ in the CTAB aqueous solutions formed entangled wormlike micelles, which led to a viscous solution. Both solutions exhibit pseudoplastic behavior characteristic of non-Newtonian fluids. Furthermore, the solution containing XGD exhibited a slightly higher viscosity at shear rates higher than 100 s^{-1}. In general, the wormlike micelle solutions exhibited a trend similar to that of the polymer suspension. This behavior is in

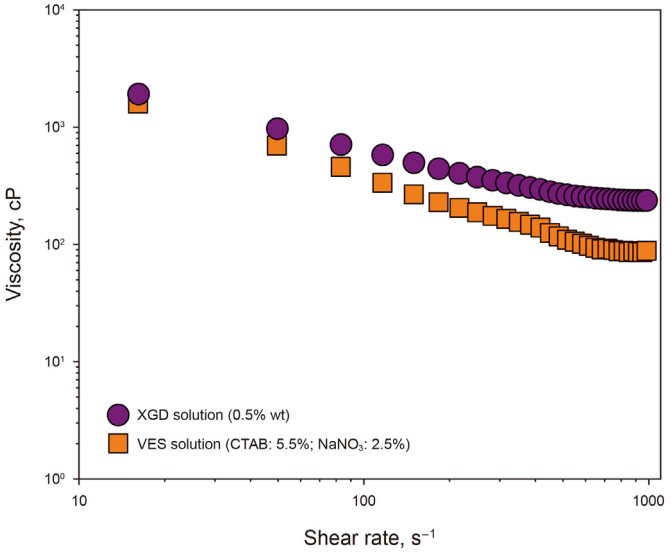

Fig. 6. Rheological behavior of XGD and VES solutions.

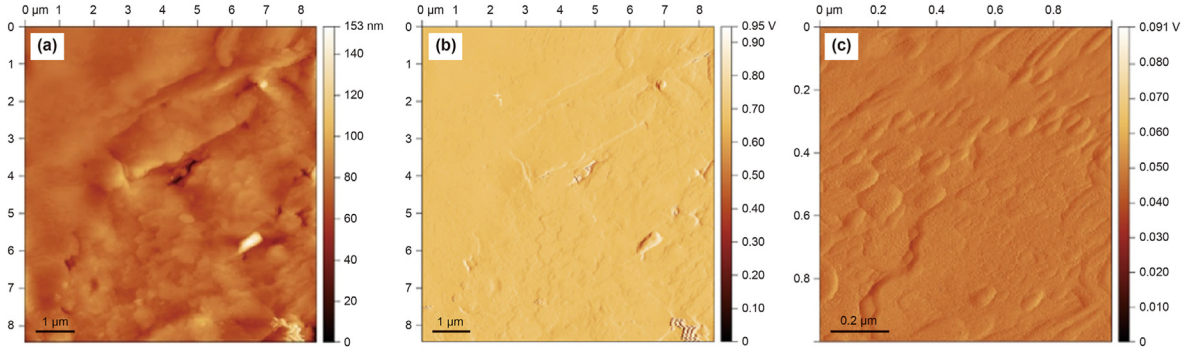

Fig. 5. Micrographs of dehydrated VES obtained by AFM. The images correspond to: (**a**) topography (8 × 8 μm), (**b**) phase (8 × 8 μm), and (**c**) amplitude (1 × 1 μm), respectively.

agreement with the results obtained by Wang et al. (2017), who found that the degree of structural alignment of worm micelles is related to the extent of pseudoplastic behavior, promoting a decrease in viscosity with increasing shear rate. Yang et al. (2022) reported that entangled wormlike micelles increase the viscosity of solutions, such as polymers, and they can break and re-form under shear. For this reason, it is sometimes called a '*living polymer*' (Yang et al., 2022).

3.2. Rheological characterization of WBMs

The results obtained from the steady and dynamic shear assays of WBMs are shown in Fig. 7. The studied WBMs exhibit pseudoplastic and viscoelastic behaviors. In particular, fluids with XGD and VES exhibited similar viscosities at high shear rates (Fig. 7(a)). However, the viscosity at a low shear rate was slightly higher for the WBMs containing VES. The pH and density of the prepared fluids are in the range of 9 ± 0.5 and 1.50 g/cm^3, respectively. In Fig. 7(b) the curves of the viscous moduli (G''), and elastic (G') for WBMs are depicted. All fluids exhibited similar viscoelastic properties. However, the WBM based on VES at frequencies below 1 Hz exhibits a G'' higher than G', indicating a liquid-like behavior. This result can be associated with the structuration degree and relaxation time of worm micelles present in the VES at low frequencies, and the surface interactions with the other WBMs components.

The viscosity of drilling fluids based on clays, polymers, and particles depends on the surface interactions between additives. Different researchers have concluded that the surface interactions between bentonite and polymers are determined by several association mechanisms, such as electrostatic interactions, hydrogen bonding, and hydrophobic interactions (Li et al., 2018a, 2018b, 2020b). Thus, the viscosity of WBMs based on VES is also related to the surface interactions between bentonite, VES, and PAC. Janek and Lagaly (2003) reported that the interaction of a cationic surfactant and bentonite is related to the surface interactions, and depending on the medium conditions, the surfactant can act as a coagulant agent for clay dispersion. It can be noted that the VES was obtained from CTAB (cationic surfactant) and $NaNO_3$. Thus, electrostatic, hydrogen bonding, and hydrophobic interactions should be considered.

Na-bentonite is a clay mineral composed of montmorillonite platelets and does not exhibit homogeneous charge distributions. Bentonite exhibited negatively charged faces related to the isomorphic substitution of lattice cations. In this study, the face and edge of the Na-bentonite were negatively and positively charged, respectively.

VES has hydrophobic chains and hydrophilic head groups. Likewise, they have a noticeable viscoelastic property associated with the creation of wormlike micelles and entangled structures above the micellar concentration. Wormlike micelles are obtained through non-covalent bonds, which lead to micelle linkage. In addition, the formed structure is temporary, which generates an entanglement-dispersion equilibrium (Hu et al., 2021). As it was previously discussed, the fluids containing VES present a slightly higher viscosity than those designed with XGD. This behavior could be associated with the several higher surface interactions of bentonite, VES, and polyanionic cellulose, and the mechanism of viscosity increase of worm-like micelles. Concerning surface interactions, the only difference in the design of WBMs is the content of XGD or VES. The Z-potential values of XGD and VES were −36 and −20 mV, respectively. The higher surface charge of XGD in WBMs is expected to produce greater electrostatic repulsion with bentonite edges and polyanionic cellulose polymer, promoting a slightly lower viscosity of WBMs based on XGD. In contrast, XGD molecules are produced by a polymerization reaction that generates high viscosity. However, viscosity is reduced by breaking the covalent bonds between the XGD molecules, leading to chain separation. In contrast, the network-like structure formed by VES through physical interactions (hydrophobic, electrostatic, and hydrogen bond interactions) increases the viscosity of the solutions and can be restored under shear. The hypothesis of the rheological properties of WBMs is in accordance with previous studies by our research group (Clavijo et al., 2021a, 2021b). These studies associated the rheological properties with hydrogen bonding, electrochemical forces, and electrostatic interactions between additives.

3.3. Effect of silica nanoparticles in the functional properties of WBMs

3.3.1. Rheological properties

In this section, the main interaction mechanisms of VES and silica nanoparticles, as well as XGD and silica nanoparticles, are considered for rheological analysis.

Fig. 8 presents the effect of the nanoparticle concentration on the rheological properties of the WBMs. The WBMs exhibit shear thinning behavior that is more noticeable for VES-based fluids. As the concentration of nanoparticles increased from 0.001 to 0.1 wt%, a slight increase in rheological properties was observed for both systems. The opposite trend was shown at 1.0 wt% nanoparticles (XGD/1.0Si and VES/1.0Si fluids). These results indicate that higher concentrations of nanoparticles saturate the WBM network structure and promote particle aggregation, which is detrimental to rheological properties. Likewise, the excess of nanoparticles causes high adsorption of the material, avoiding free material for viscoelastic network formation. These results are in accordance with those reported by Clavijo et al. (2021b) who studied the theoretical

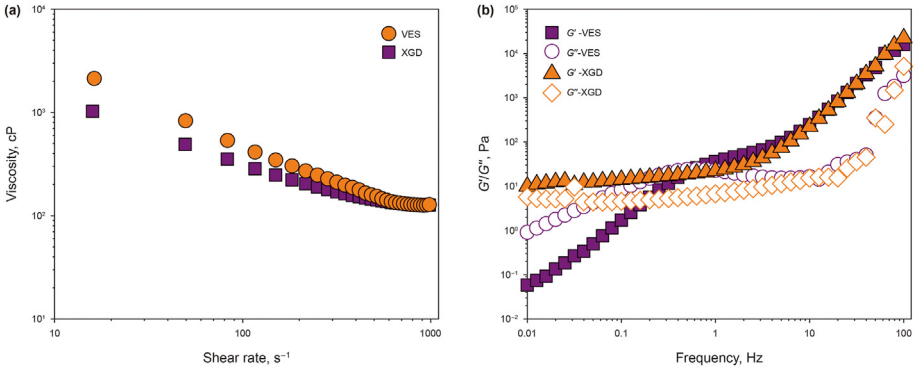

Fig. 7. Rheological behavior of XGD-based and VES-based WBM: (**a**) flow curve and, (**b**) mechanical spectra.

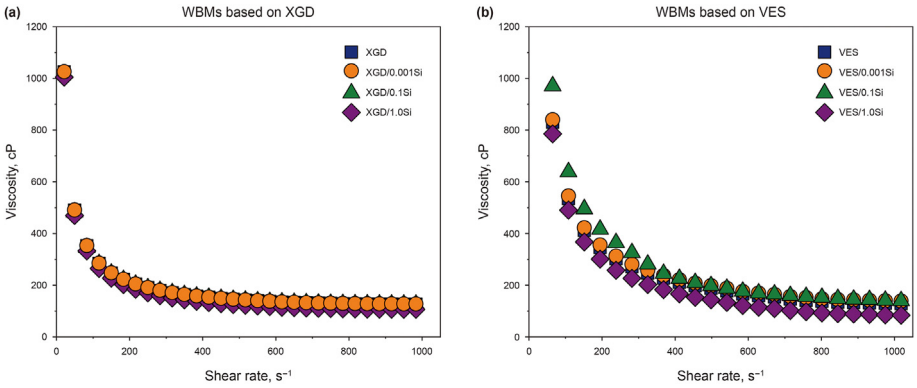

Fig. 8. Effect of nanoparticle concentration in the rheological behavior of WBMs: (**a**) WBMs based on VES, and (**b**) WBMs based on XGD.

and experimental interactions among silica nanoparticles, $CaCO_3$, and xanthan gum as additives in WBMs. Through molecular simulations, they found that xanthan gum and silica nanoparticles interacted via hydrogen bonding between the silanol and carboxylate groups. Thus, this interaction increased the thermal stability of the polymer. In general, nanoparticles act as points between the polymer chains, promoting the viscoelastic structure of the WBMs. In contrast, the concentration 0.1 wt% was reported as optimum concentration of NP. In contrast, concentrations higher than this value deteriorate the properties due to agglomeration.

As reported in the literature, VES can interact with several nanoparticles independently of their size, shape, and surface groups (Philippova and Molchanov, 2019). The interaction begins with the covering of the surface of nanoparticles with adsorbed surfactants. The structure of surfactant aggregates formed on the surface of the nanomaterial is determined by the nature of the surfactant and its interaction surface. When nanoparticles are oppositely charged with respect to the surfactant ions (as is the case in this work), the electrostatic interactions govern and the surfactant is adsorbed on the nanoparticle through its charged head groups (Philippova and Molchanov, 2019). The end-caps of micelles are considered to participate in the interaction, promoting cross-linking of micelles (Wang et al., 2017). This behavior generates a network structure that increases the viscosity of WBMs. However, at higher nanoparticle concentrations, the decrease in viscosity could be associated with interparticle aggregation, which promotes disruption of the network structure. Furthermore, it should be considered that the adsorption of the surfactant molecules on the surface of nanoparticles can reduce the amount of surfactant involved in the formation of VES. This effect was observed in WBMs containing 1.0 wt% silica nanoparticles. Fig. 9 shows the possible surface interaction between the VES and silica nanoparticles.

As mentioned previously, the microstructure of WBMs (clay, polymer, and worm micelles or VES and nanoparticles) is governed by the connection mode of clay, charge and size of nanoparticles, chemical structure of the polymer and VES, and mechanism of viscosity increase, which promotes changes in the rheological properties of WBMs. Overall, the results of the enhanced viscosity of fluids are mainly determined by the surface interactions of the worn micelles with silica nanoparticles, Na-bentonite, and PAC polymer, forming a pseudo-crosslinking microstructure. Thus, the reorganization of the micellar structure of worm micelles on WBMs promotes a significant change in the rheological properties of fluids with VES. Helgeson et al. (2010) studied the rheology of cationic worm-like micelles with negatively charged nanoparticles. The authors argued that the creation of micelle-nanoparticle junctions acts as physical cross-links, promoting high viscosity and elasticity in dilute and semi-dilute wormlike micelles (Kang et al., 2020).

3.3.2. Rheological models

The Herschel-Bulkley model was adjusted, and the results were compared with the experimental data. It can be observed that fluids exhibit the behavior of the Herschel-Bulkley model under the evaluated conditions. Table 2 lists the model parameters and experimental errors associated with the adjustment. Fig. 10 shows a comparison between the results of the Herschel-Bulkley model and

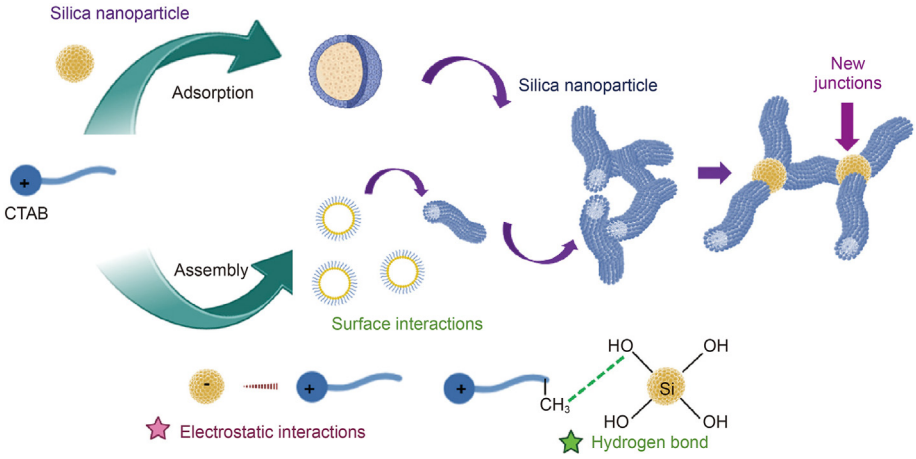

Fig. 9. Schematic representation of the interactions between VES and silica nanoparticles.

Table 2
Parameters[a] of the Herschel Buckley model for studied WBMs.

Group	Fluid	Nanoparticles, wt%	τ_0, Pa	k , Pa s^{-1}	n	RSMD	R^2
Based on XGD	XGD	0.00	12.74	0.43	0.80	0.11	0.99
	XGD/0.001Si	0.01	18.99	0.15	0.94	0.02	0.99
	XGD/0.1Si	0.10	12.44	0.43	0.80	0.11	0.99
	XGD/1.0Si	1.00	19.08	0.13	0.93	0.03	0.98
Based on VES	VES	0.00	30.04	0.63	0.67	0.02	0.99
	VES/0.001Si	0.01	39.54	0.73	0.70	0.01	0.99
	VES/0.1Si	0.10	45.28	1.35	0.60	0.13	0.97
	VES/1.0Si	1.00	31.88	0.16	0.36	0.04	0.97

[a] Correlation coefficient (R^2); yield stress, τ_0 (Pa); consistency index, k (Pa s^{-1}); flow behavior index; root-mean-square deviation (RSMD).

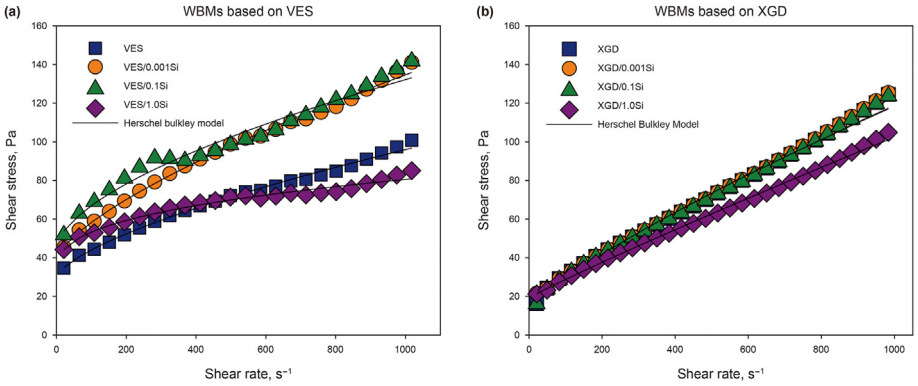

Fig. 10. Effect of nanoparticles concentration in the rheological behavior of WBMs: (**a**) WBMs based on VES, and (**b**) WBMs based on XGD. Solid lines represent the Herschel Buckley model simulation.

experimental data. Herschel Bulkley's model accurately fitted the data and revealed a non-Newtonian and pseudoplastic behavior, with the "n" parameter. A higher consistency index (k) corresponds to the WBMs based on VES, verifying the higher rheological properties than those based on XGD. The yield stress (τ_0) increased with the silica nanoparticle concentration for all the fluids. However, the higher τ_0 values correspond again to the WBMs based on VES. These results were consistent with those obtained from the flow curves (Fig. 8).

3.4. Filtration properties

Owing to the differential pressure in the well, the water contained in the WBMs flowed into the formation during the drilling operation. This causes clay swelling and leads to damage to the formation. The application of high pressure during drilling facilitates the deposition of bentonite platelets and solid particles, resulting in the creation of a layer called a "filter cake." This filter cake acted as a barrier, impeding the penetration of water into the formation.

The properties of the filter cake, such as thickness, filtration rate, and permeability fulfill an important role in preventing water invasion into the cake formation. Thus, high-performance WBM formulations require low fluid loss volume and the formation of a compact, impermeable, and thin filter cake.

Figs. 11–13, and Table 3 show the filtration properties of the evaluated WBMs. The filtration properties were evaluated for fluids without nanoparticles (VES and XGD WBMs) and fluids containing several concentrations of nanoparticles. In Fig. 11, the curves of the filtrate volume *vs* time for the WBMs based on VES and XGD are compared. Fluids based on VES showed lower filtrate volumes. In comparison with fluids without nanoparticles, a notable impact of

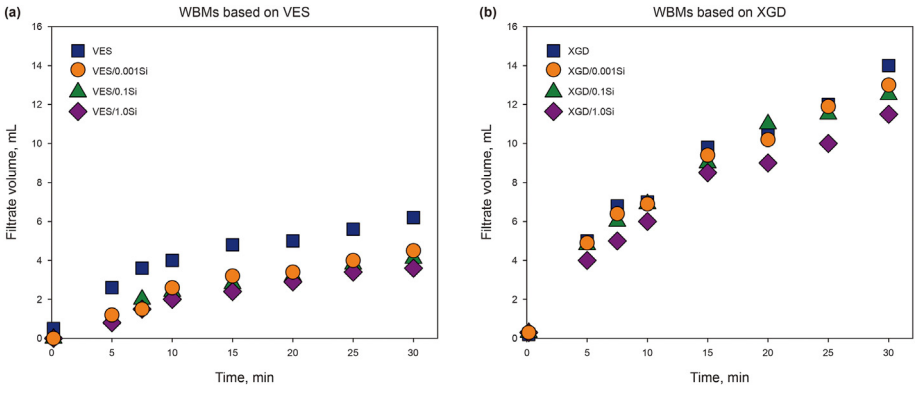

Fig. 11. Filtration properties of WBM at low-pressure and low-temperature (LTLP) conditions: (**a**) WBMs based on VES, and (**b**) WBMs based on XGD.

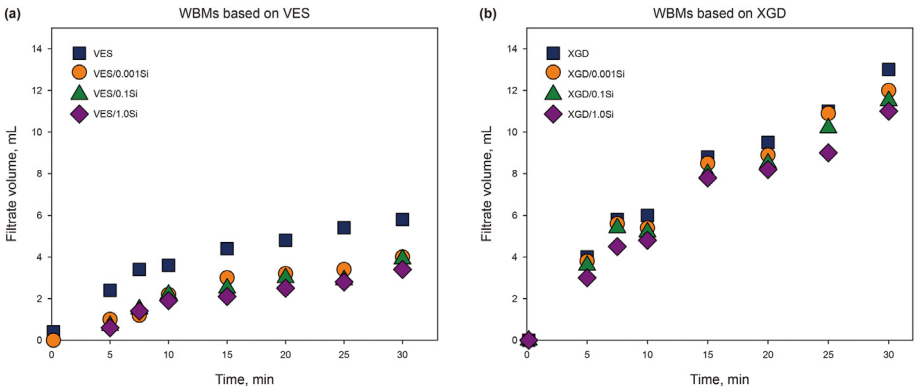

Fig. 12. Filtration properties of filter cake performance at LTLP) conditions: (**a**) WBMs based on VES, and (**b**) WBMs based on XGD.

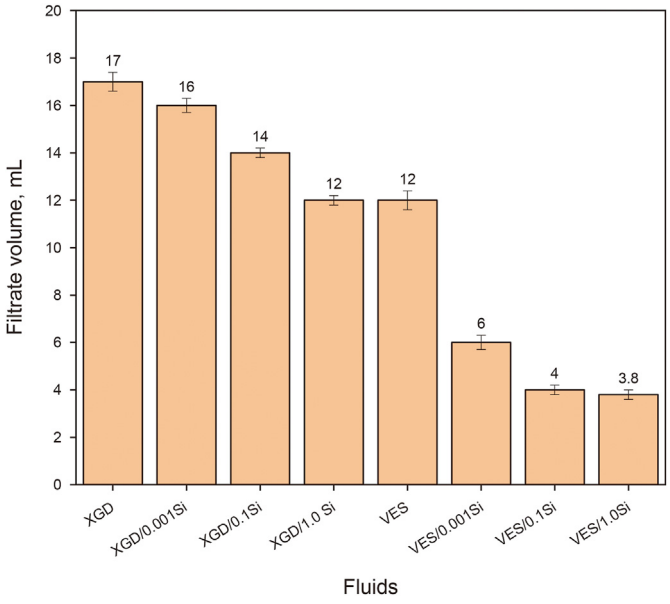

Fig. 13. Filtrate volume at 30 min, obtained from HTHP conditions for studied fluids.

Table 3
Filtration properties of filter cakes. The liquid flowing through the already formed cake method was considered to determine the filtration rate, as reported previously (Li et al., 2018a).

Fluid	$q \times 10^{-2}$, m^3/seg[a]	t_c, cm[a]	$K_c \times 10^{-6}$[a]
VES	0.69	0.15	2.75
VES/0.001Si	0.51	0.14	2.38
VES/0.1Si	0.52	0.13	2.40
VES/1.0Si	0.43	0.12	2.16
XGD	1.37	0.15	5.46
XGD/0.001Si	1.38	0.14	5.96
XGD/0.1Si	1.29	0.13	6.00
XGD/1.0Si	1.02	0.13	5.07

[a] The error for the measurements was ±0.01.

silica nanoparticles on the decrease in the filtrate volume was observed for both fluid groups.

The filtrate volume at a high concentration of nanoparticles for the fluids containing VES or XGD is 2.5 and 10 mL, respectively (fluids VES/1.0Si and XGD/1.0Si). The reduction in filtrate volume can be related to the fact that a higher nanoparticle concentration acts as a cell and fills the filter cake pores. According to the results of the molecular simulation for the WBMs filtration properties reported by Clavijo et al. (2021b), the presence of silica nanoparticles decreases the repulsive interaction energy between the WBMs components.

Fig. 12 shows the filtration characteristics of the filter cake. The presence of silica nanoparticles led to a reduction in the filtrate volume for all evaluated filter cakes. This behavior is more noticeable for the filter cake based on the VES. In particular, the filtrate volumes for filter cakes obtained from fluid VES and XGD at 30 min were 4.6 and 12 mL, respectively. In the presence of silica nanoparticles in the filter cake, the volume of the filtrate was reduced to 2 and 10 mL for the VES/1.0Si and XGD/1.0Si fluids, respectively.

The properties of the filter cakes, such as thickness, filtrate rate, and permeability, for the WBMs are shown in Table 3. The concentration of silica nanoparticles decreased the thickness, permeability, and filtrate rate of the filter cake. This result indicates that the nanoparticles promoted the formation of a more compact structure with a uniform distribution of additives in the filter cake. In general, fluids containing VES exhibit lower filtration rates and permeabilities. The thickness of the filter cake exhibited the same behavior with the addition of nanoparticles. It is important to note that these results are related to the evaluation of the filter cake performance. In this sense, the results are similar to those of the filtration volume. Compared with the filtrate volume after filter cake formation, the filtrate cake is expected to avoid flow, and the filtrate volume will be lower.

Fig. 13 shows the filtrate volume for the filtration test under HTHP conditions. The filtrate volume decreased with the nanoparticle concentration for all evaluated fluids. Again, this behavior is more noticeable for fluids based on VES. However, the effect of a higher nanoparticle concentration on the reduction of the filtrate volume for the fluid VES/1.0Si is not significant for VES/0.1Si. This result can be related to the saturation of the filter cakes with high concentrations of nanoparticles at high temperatures, promoting their agglomeration.

As expected and reported in the literature (Li et al., 2018a, 2020b; Villada et al., 2018, 2022), the filtration properties of WBMs are influenced by the surface interactions of bentonite, polymer, VES, and silica nanoparticles, the formation of filter cake, the microstructure of the filter cake (compact, dense, or loose), filter cake porosity, rheological properties, and operating conditions. Several authors have found that the filtrate volume depends on the filter cake performance (Li et al., 2020b; Mahto and Sharma, 2004). Overall, a low filtrate volume is obtained with the formation of a thin, compact, and impermeable filter cake, whereas a high filtrate volume is associated with the creation of a thick, loosened, and permeable filter cake (Villada et al., 2022).

By comparing the filtration properties of the fluids designed

containing VES or XGD polymers, enhanced filtration properties were observed for the WBMs based on VES. These results were in accordance with the rheological properties discussed above. Hence, fluids with higher viscosity exhibited a low filtration volume. Because of the negative charges of XGD, VES, and nanoparticles, nanoparticles are very dispersed and homogeneously distributed in the structure formed by bentonite platelets, cellulose polyanionic polymers, XGD polymers, or VES, allowing the obturation of small pores in the filter cake. However, the significant difference in the filtration properties of WBMs based on VES could be associated with the higher interaction of VES with bentonite, polymers, and nanoparticles, and mainly with the physicochemical configuration of VES and its adsorption on nanoparticles (Huang et al., 2022). As a result, VES could be restructured and linked to the nanoparticles through free end-caps forming junction points that promote an entanglement structure more compact than those formed by XGD. This result is in accordance with the SEM images. XGD is the most commonly used polymer as a viscosifier additive in drilling fluids owing to the enhancement of rheological and filtration properties as a consequence of surface interactions (electrostatic interaction, hydrogen bonding, and hydrophobic interactions) with other WBMs components. To compare the results with VES, it is necessary to consider the physicochemical formation and degree of structural dynamics of VES that promote the modification of the rheological and filtration properties. Intra-micelle (micelle-to-micelle) pseudo-crosslinking builds with nanoparticles to generate a much stronger dynamic micelle network. Villada et al. (2022) studied WBMs based on XGD, bentonite, polyanionic cellulose, and $CaCO_3$ particles. The improvement in the rheological and filtration properties depends on the superficial interactions between the polymeric additives (XGD, PAC), clay (bentonite), and calcium carbonate particles. Hence, the homogenous distribution of the particles in the matrix formed by bentonite and polymers increases the viscosity and lowers the filtrate volume.

3.5. Structural properties

Fig. 14 depicts the micrographs obtained through SEM of the WBMs design for the base fluid XGD, VES (without nanoparticles), and fluids XGD/1.0, VES/1.0Si containing nanoparticles at a concentration of 0.1 wt%. The micrographs suggest the formation of two different microstructures for the WBMs and a significantly different network structure. In particular, the base fluid containing VES exhibited the presence of an agglomerate with a homogeneous distribution (Fig. 14(a) and (b)). Magnification of image at 10.000X (Fig. 12(b)) could suggest the bentonite intercalation with the wormlike micelles and the presence of polyanionic cellulose as polymeric films that generate a more compact structure. The micrograph for fluid VES/1.0Sicontaining silica nanoparticles (Fig. 14(c)), shows that the nanoparticles are distributed along the WBMs microstructure. It can be observed that the nanoparticles appear to be embedded in the worm-like structure of the VES, promoting a network structure. The micrographs for the fluid XGD (Fig. 14(d)) show the bentonite coating with polymeric films observed at image magnification (Fig. 14(e)). Likewise, the nanoparticles appeared to be homogenously distributed in the WBM microstructure (Fig. 14(f)). However, the microstructure formed for XGD and other additives is looser, promoting weak interactions between XGD, BT platelets, and polyanionic cellulose.

In general, a more compact laminar structure was observed for WBMs based on VES, confirming the higher surface interactions of VES with bentonite, polyanionic cellulose, and nanoparticles. In contrast, the microstructure of the WBMs containing XGD exhibited a spherical structure. In all cases, the nanoparticles promoted the formation of a denser filter cake with high packing among the particles, thereby avoiding the presence of pores and cracks. These results are in accordance with those of previous studies, which suggested that the adsorption of nanoparticles is determined by London, double layer, and hydrodynamic forces. Likewise, nanoparticles fill the space between the bentonite particles and the interlayers, reducing the filtration volume. This result is consistent with that obtained with the filter properties (Fig. 11), where the presence of silica nanoparticles promoted the formation of a more compact filter cake.

3.6. Thermal properties

Fig. 15 shows the thermal stabilities of the studied WBMs. The

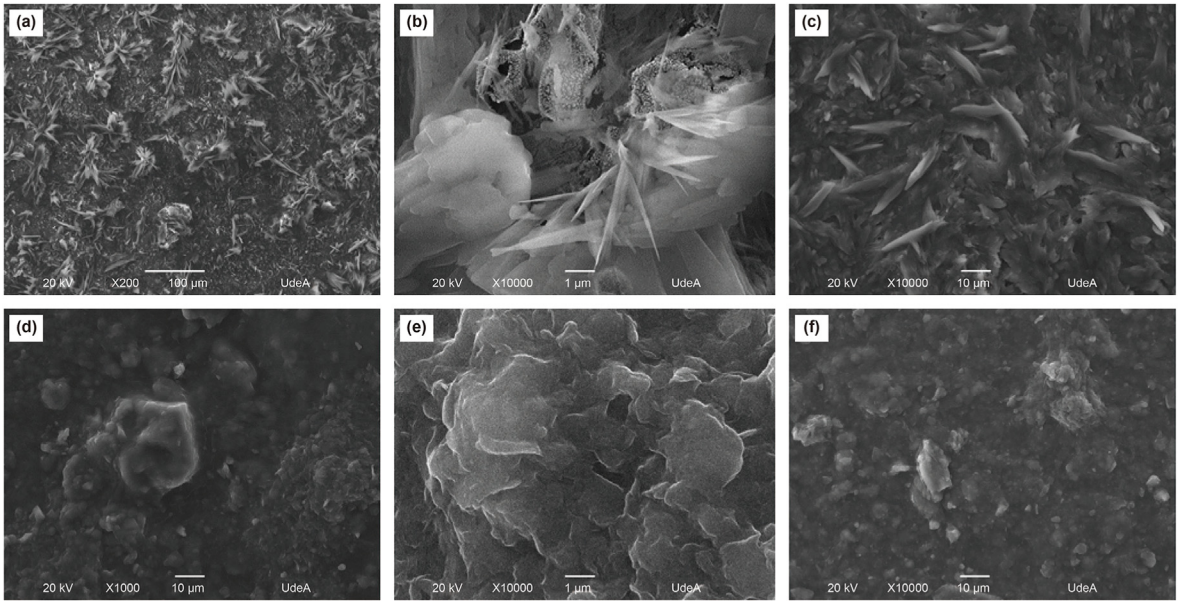

Fig. 14. Micrographs of WBMs obtained by SEM: (**a**–**c**) WBMs based on VES; (**d**–**f**) WBMs based on XGD. The effect of silica nanoparticles (0.1 wt %) in the structure of WBMs is present in the micrograph (**c**) and (**f**).

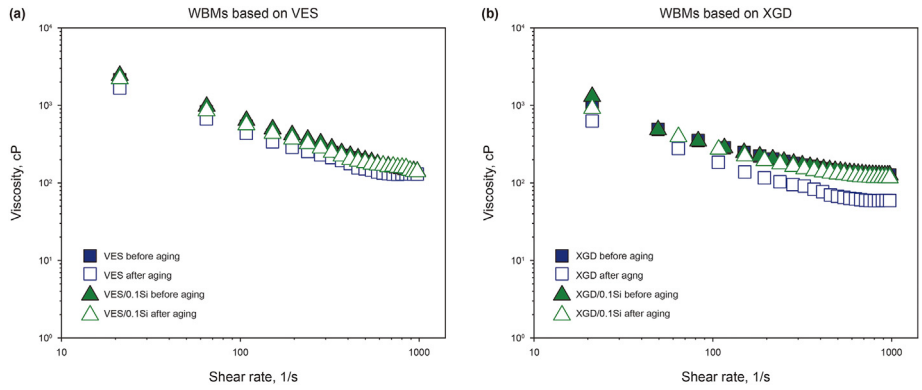

Fig. 15. Thermal stability of WBMs conditions: (**a**) fluids without nanoparticles, and (**b**) fluids containing nanoparticles. The rheological properties were determined before and after aging.

stability of the WBMs was evaluated based on their rheological properties before and after thermal treatment. Considering the preliminary results, XGD, XGD/0.1Si, VES, and VES/0.1Si were selected for this study. Note that fluids XGD and VES are the base fluids without nanoparticles, and fluids XGD/0.1Si and VES/0.1Si contain 0.1 wt % of silica nanoparticles. It can be observed that the WBMs based on VES exhibited slight changes in viscosity before and after the aging test. With respect to the stability of WBMs based on XGD, a significant effect was observed for the fluid without nanoparticles. In general, nanoparticles improve the thermal stability of the WBMs. These results can be related to the mechanism of interaction between VES and nanoparticles. This mechanism is related to the formation of pseudo-cross-linking, which functions as physical cross-linking among micelles when the micelles junction with the nanoparticles. Thus, viscoelasticity can be improved at high temperatures. These observations are in accordance with those reported by Mao et al. (2018), who investigated the use of nanoparticles to improve the heat resistance of a VES. Likewise, the TGA analysis of VES indicates high thermal stability up to ~260 °C, and the thermogram published by Villada et al. (2022) for XGD shows polymer degradation at 268 °C. Therefore, the differences in the rheological properties of fluids after thermal aging are not associated with polymer, VES, or nanoparticle degradation. This result again shows that the addition of silica nanoparticles promotes the thermal stability of WBMs based on VES, owing to the higher interaction between VES and the nanoparticles and other WBMs components, as previously discussed in the rheological properties section.

3.7. Micromodel analysis

Considering the filtration properties, two WBMs containing VES were selected for analysis. Figs. 16 and 17 show the evolution of filtrate volume with time in the micromodel. Notably, the micromodel was initially saturated with crude oil to simulate the formation conditions before the drilling process. The evolution of the filtrate volume with time for the WBMs based on VES (without nanoparticles) in the porous medium is presented in Fig. 16. Slight changes were observed in the micromodel at the beginning of fluid injection (Fig. 16(a)). During WBM injection, a displacement of the oil by the fluid following a homogeneous distribution was observed (Fig. 16(b)). The images 16(c) and (d) suggest the presence of slight emulsions and a possible internal filter after 10 min of WBM injection. Images (e) and (f) (Fig. 16) show the total invasion of fluid into the porous medium at 281 min, achieving a filtrate volume of 0.35 mL. Likewise, the fluid invaded the right zone of the micromodel with no homogeneity. Fig. 17 shows the images of the filtrate volume evolution with time for the fluid VES/0.1Si (containing 0.1 wt% of nanoparticles) in the porous medium. Oil displacement was not observed in the presence of WBM at the beginning of the

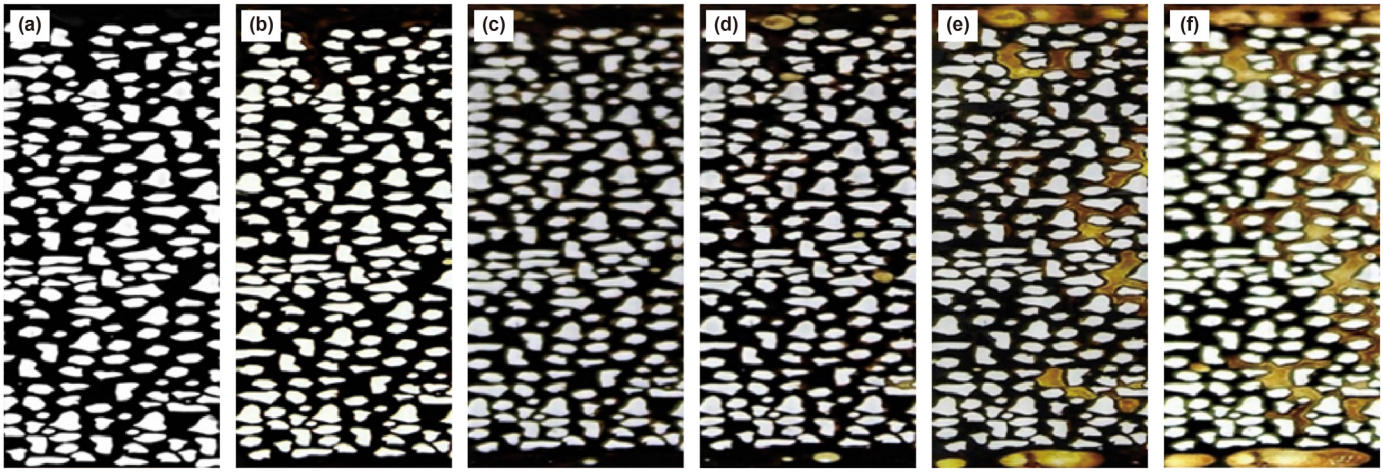

Fig. 16. Photographs showing the evolution of filtrate volume with time in the micromodel for WBM based on VES without silica nanoparticles at: (**a**) 0, (**b**) 10, (**c**) 35, (**d**) 68, (**e**)167, (**f**) 281min. The assays were performed using a micromodel device.

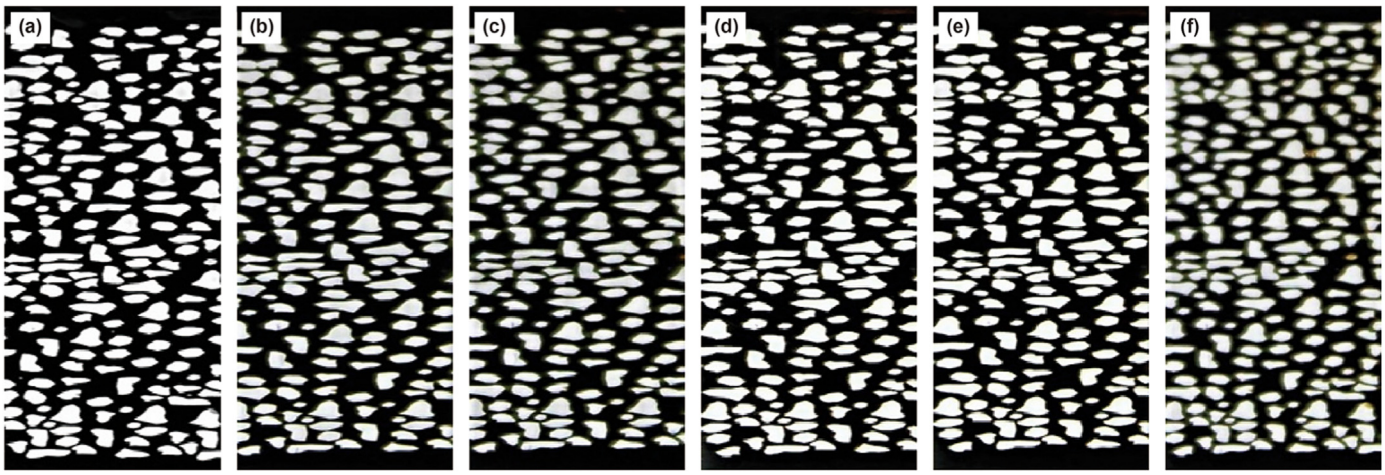

Fig. 17. Photographs for the evolution of filtrate volume with time in the micromodel for fluid (VES/0.1) contains silica nanoparticles at: (**a**) 0, (**b**) 10, (**c**) 35, (**d**) 68, (**e**)167, (**f**) 281min. The assays were performed using a micromodel device.

fluid injection (Fig. 17(a)–(c)). In contrast, Fig. 17(d)–(f) show the displacement of crude oil and the formation of small micro-emulsions. The filtrate volume achieved at 281 min was 0.04 mL, indicating that the presence of nanoparticles reduced the filtrate volume.

Compared with the images of the micromodel for fluids in the absence and presence of nanoparticles, it was observed that the nanoparticles reduced the penetration depth of mud into the micromodel through external and internal plugging mechanisms. Likewise, nanoparticles can decrease the formation of emulsions on the pore surface, modifying the wettability of the micromodel to a more water-wetting state. However, this observation was not clear in the images. These results are in accordance with the filtrate volume achieved in the presence of nanoparticles from the static filtration results previously discussed. Mohammadi and Mahani (2020) investigated the pore-scale mechanisms of the formation damage promoted by mud in the presence of nanomaterials using a microfluidic approach. The results indicate that the incorporation of nanoparticles reduced the penetration depth of the drilling fluid in the micromodel.

Considering the previous results, the use of VES in the formulation of WBMs improved their functional properties. However, the presence of silica nanoparticles at 0.1 wt% remarks this effect related to the synergistic interactions with the VES. According to (Saleh, 2018), the more significant effects of nanomaterials on the functional properties of WBMs are related to the surface interactions between additives. In general, nanomaterials improve the rheological properties of WBMs through numerous mechanisms, depending on the characteristics of the NPs and the continuous phase of the drilling fluid. Likewise, NPs inhibit the penetration of fluid into formations, avoiding shale swelling and filtration loss. Silica nanomaterials also enhance the thermal stability of WBMs owing to the presence of oxides in the chemical structure, which inhibit the degradation of polymeric chains with increasing temperature. Likewise, nanosilica improves the lubricity of WBMs by forming a boundary-type system via the adhesion of nanoparticles over the metal surface. It is important to note that the lubricity of WBMs depends on the viscosity and the colloidal stability of the nanofluids (Katende et al., 2019).The obtained results showed that the silica nanoparticles improve the rheological, filtration, and thermal properties of WBMs. This behavior is more noticeable for WBMs based on VES. Specifically, the viscosity slightly increases in the presence of nanomaterials, allowing optimization of the fluid composition. Regarding the filtrate volume and thermal stability, the nanoparticles contributed to decreasing the filtrate volume and reducing the mudcake permeability as well as the thermal stability of the nanofluids. The impact on these parameters is related to the different interaction mechanisms between the WBMs components. On the other hand, the limitations of this research are related to the evaluation of the properties at high temperatures (above 120 °C) considering the evaporation of aqueous base of fluid. However, the results obtained are very promising and can be applied to harsh conditions.

4. Conclusions

The use of VES as a possible replacement for XGD in WBM formulations was evaluated. Specifically, VES was performed using CTAB and $NaNO_3$ and characterized in terms of charge surface, rheological properties, thermogravimetric analysis, and morphology. The VES characterization results showed a negative surface charge, shear thinning behavior, high thermal stability, and cylindrical morphological structure. Regarding the replacement of XGD, the results suggested that VES has properties as a rheology modifier or filtration agent in WBMs under high-temperature conditions. Similarly, VES can be applied in WBMS as a replacement for XGD polymers. Fluids containing VES and silica nanoparticles at 0.1 wt % exhibited superior functional properties, associated with the specific characteristics of the viscosity increase mechanism of VES, as well as their interaction with bentonite, polyanionic cellulose, and nanoparticles. The filtrate volume at the LTLP and HTHP decreased with the addition of nanoparticles in all the fluids. The formation damage was reduced with the presence of silica nanoparticles at 0.1 wt% in the WBMs based on VES. A techno-economic assessment and the use of VES with different chemical natures will be the subject of future communications to evaluate the application of VES in drilling fluids.

CRediT authorship contribution statement

Yurany Villada: Writing – review & editing, Writing – original draft, Visualization, Validation, Methodology, Investigation, Formal analysis, Data curation, Conceptualization. **Lady Johana Giraldo:** Methodology, Formal analysis, Conceptualization. **Carlos Cardona:** Software, Investigation. **Diana Estenoz:** Writing – review & editing, Supervision. **Gustavo Rosero:** Software, Methodology. **Betiana**

Lerner: Visualization, Software. **Maximiliano S. Pérez:** Visualization, Validation, Software. **Masoud Riazi:** Visualization, Supervision. **Camilo A. Franco:** Writing – review & editing, Visualization, Supervision, Resources, Project administration, Formal analysis, Conceptualization. **Farid B. Córtes:** Writing – review & editing, Visualization, Supervision, Resources, Project administration, Formal analysis.

Declaration of competing interest

The authors declare that they have no known competing financial interests or personal relationships that could have appeared to influence the work reported in this paper.

Acknowledgements

This study was funded by Fondo Francisco José de Caldas, MINCIENCIAS and Agencia Nacional de hidrocarburos (ANH) through contract No. 112721-282-2023 (Project 1118-1035-9300) with Universidad Nacional de Colombia - Sede Medellín and PAREX RESOURCES COLOMBIA AG SUCURSAL

Appendix A. Supplementary data

Supplementary data to this article can be found online at https://doi.org/10.1016/j.petsci.2024.11.014.

References

Abdullah, A.H., Ridha, S., Mohshim, D.F., Yusuf, M., Kamyab, H., Krishna, S., Maoinser, M.A., 2022. A comprehensive review of nanoparticles: effect on water-based drilling fluids and wellbore stability. Chemosphere 308, 136274. https://doi.org/10.1016/j.chemosphere.2022.136274.

Aftab, A., Ali, M., Arif, M., Panhwar, S., Saady, N.M.C., Al-Khdheeawi, E.A., Mahmoud, O., Ismail, A.R., Keshavarz, A., Iglauer, S., 2020. Influence of tailor-made TiO_2/API bentonite nanocomposite on drilling mud performance: towards enhanced drilling operations. Appl. Clay Sci. 199, 105862. https://doi.org/10.1016/j.clay.2020.105862.

Agista, M.N., Guo, K., Yu, Z., 2018. A state-of-the-art review of nanoparticles application in petroleum with a focus on enhanced oil recovery. Appl. Sci. 8 (6), 871. https://doi.org/10.3390/app8060871.

Ali, I., Ahmad, M., Ganat, T., 2022. Biopolymeric formulations for filtrate control applications in water-based drilling muds: a review. J. Pet. Sci. Eng. 210, 110021. https://doi.org/10.1016/j.petrol.2021.110021.

Ali, J.A., Abbas, D.Y., Abdalqadir, M., Nevecna, T., Jaf, P.T., Abdullah, A.D., Rancová, A., 2024a. Evaluation the effect of wheat nano-biopolymers on the rheological and filtration properties of the drilling fluid: towards sustainable drilling process. Colloids Surf. A Physicochem. Eng. Asp. 683, 133001. https://doi.org/10.1016/j.colsurfa.2023.133001.

Ali, J.A., Abdalqadir, M., Najat, D., Hussein, R., Jaf, P.T., Simo, S.M., Abdullah, A.D., 2024b. Application of ultra-fine particles of potato as eco-friendly green additives for drilling a borehole: a filtration, rheological and morphological evaluation. Chem. Eng. Res. Des. 206, 89–107. https://doi.org/10.1016/j.cherd.2024.04.051.

Alsaba, M., Al Marshad, A., Abbas, A., Abdulkareem, T., Al-Shammary, A., Al-Ajmi, M., Kebeish, E., 2020. Laboratory evaluation to assess the effectiveness of inhibitive nano-water-based drilling fluids for Zubair shale formation. J. Pet. Explor. Prod. Technol. 10, 419–428. https://doi.org/10.1007/s13202-019-0737-3.

Al-Yasiri, M., Awad, A., Pervaiz, S., Wen, D., 2019. Influence of silica nanoparticles on the functionality of water-based drilling fluids. J. Pet. Sci. Eng. 179, 504–512. https://doi.org/10.1016/j.petrol.2019.04.081.

Anderson, R.W., Baker, J.R., 1974. Use of guar gum and synthetic cellulose in oilfield stimulation fluids. Fall Meeting of the Society of Petroleum Engineers of AIME. Houston, Texas. https://doi.org/10.2118/5005-MS.

Bao, X.N., Zhang, W.D., Gang, H.Z., Yang, S.Z., Li, Y.C., Mu, B.Z., 2021. Formation of viscoelastic micellar solutions by a novel cationic surfactant and anionic salt system. Colloids Surf. A Physicochem. Eng. Asp. 611, 125795. https://doi.org/10.1016/j.colsurfa.2020.125795.

Blkoor, S.O., Norddin, M.N.A.M., Ismail, I., Oseh, J.O., Risal, A.R., Basaleh, S.S., Mohamed, M.H., Duru, U.I., Ngouangna, E.N., Yahya, M.N., 2023. Enhanced cutting transport performance of water-based drilling muds using polyethylene glycol/nanosilica composites modified by sodium dodecyl sulphate. Geoene. Sci. Eng. 230, 212276. https://doi.org/10.1016/j.geoen.2023.212276.

Caenn, R., Chillingar, G.V., 1996. Drilling fluids: state of the art. J. Pet. Sci. Eng. 14, 221–230. https://doi.org/10.1016/0920-4105(95)00051-8.

Carico, R.D., Bagshaw, F.R., 1978. Description and use of polymers used in drilling, workovers, and completions. SPE Production Technology Symposium, Hobbs. New Mexico. https://doi.org/10.2118/7747-MS.

Clavijo, J.V., Roldán, L.J., Castellanos, D.A., Cotes, G.A., Forero, Á.M., Franco, C.A., Cortés, F.B., 2021a. Double purpose drilling fluid based on nanotechnology: drilling-induced formation damage reduction and improvement in mud filtrate quality. In: Nanoparticles: an Emerging Technology for Oil Production and Processing Applications. Springer, Cham, pp. 381–405. https://doi.org/10.1007/978-3-319-12051-5_11.

Clavijo, J.V., Moncayo-Riascos, I., Husein, M., Lopera, S.H., Franco, C.A., Cortes, F.B., 2021b. Theoretical and experimental approach for understanding the interactions among SiO_2 nanoparticles, $CaCO_3$, and xanthan gum components of water-based mud. Energy Fuel. 35 (6), 4803–4814. https://doi.org/10.1021/acs.energyfuels.0c03898.

Dias, F.T.G., Souza, R.R., Lucas, E.F., 2015. Influence of modified starches composition on their performance as fluid loss additives in invert-emulsion drilling fluids. Fuel 140, 711–716. https://doi.org/10.1016/j.fuel.2014.09.074.

Elfeky, S.A., Mahmoud, S.E., Youssef, A.F., 2017. Applications of CTAB modified magnetic nanoparticles for removal of chromium (VI) from contaminated water. J. Adv. Res. 8, 435–443. https://doi.org/10.1016/j.jare.2017.06.002.

Ezell, R.G., Ezzat, A.M., Horton, D., Partain, E., 2010. State of the Art Polymers Fulfill the Need for High Temperature Clay-free Drill-In and Completion Fluids.

Fakoya, M.F., Shah, S.N., 2017. Emergence of nanotechnology in the oil and gas industry: emphasis on the application of silica nanoparticles. Petroleum 3 (4), 391–405. https://doi.org/10.1016/j.petlm.2017.03.001.

Franco, Camilo A., Franco, Carlos A., Zabala, R.D., Bahamón, Í., Forero, Á., Cortés, F.B., 2021. Field applications of nanotechnology in the oil and gas industry: recent advances and perspectives. Energy Fuel. 35 (23), 19266–19287. https://doi.org/10.1021/acs.energyfuels.1c02614.

Gao, C., 2015. Potential of welan gum as mud thickener. J. Pet. Explor. Prod. Technol. 5, 109–112. https://doi.org/10.1007/s13202-014-0114-1.

Gautam, S., Guria, C., Rajak, V.K., 2022. A state of the art review on the performance of high-pressure and high-temperature drilling fluids: towards understanding the structure-property relationship of drilling fluid additives. J. Pet. Sci. Eng. 213, 110318. https://doi.org/10.1016/j.petrol.2022.110318.

Gurluk, M.R., Nasr-El-Din, H.A., Crews, J.B., 2013. Enhancing the performance of viscoelastic surfactant fluids using nanoparticles. EAGE Annual Conference & Exhibition Incorporating SPE Europec. London, UK. https://doi.org/10.2118/164900-MS.

Hall, L.J., Deville, J.P., Santos, C.M., Rojas, O.J., Araujo, C.S., 2018. Nanocellulose and biopolymer blends for high-performance water-based drilling fluids. 2010 AADE Fluids Conference and Exhibition Held at the Hilton Houston North, Houston, Texas. https://www.aade.org/application/files/4015/7261/8004/AADE-10-DF-HO-01.pdf.

Hamed, S.B., Belhadri, M., 2009. Journal of Petroleum Science and Engineering Rheological properties of biopolymers drilling fl uids. J. Pet. Sci. Eng. 67, 84–90. https://doi.org/10.1016/j.petrol.2009.04.001.

Helgeson, M.E., Hodgdon, T.K., Kaler, E.W., Wagner, N.J., Vethamuthu, M., Ananthapadmanabhan, K.P., 2010. Formation and rheology of viscoelastic "double networks" in wormlike micelle-nanoparticle mixtures. Langmuir 26, 8049–8060. https://doi.org/10.1021/la100026d.

Huang, Z., Mao, Jincheng, Cun, M., Yang, X., Lin, C., Zhang, Y., Zhang, H., Mao, Jinhua, Wang, Q., Zhang, Q., Chen, A., Zhang, W., Zhou, H., He, Y., Liu, B., Xiao, Y., 2022. Polyhydroxy cationic viscoelastic surfactant for clean fracturing fluids: study on the salt tolerance and the effect of salt on the high temperature stability of wormlike micelles. J. Mol. Liq. 366, 120354. https://doi.org/10.1016/j.molliq.2022.120354.

Hu, R., Tang, S., Mpelwa, M., Jiang, Z., Feng, S., 2021. Research progress of viscoelastic surfactants for enhanced oil recovery. Energy Explor. Exploit. 39 (4), 1324–1348. https://doi.org/10.1177/0144598720980209.

Janek, M., Lagaly, G., 2003. Interaction of a cationic surfactant with bentonite: a colloid chemistry study. Colloid Polym. Sci. 281, 293–301. https://doi.org/10.1007/s00396-002-0759-z.

Kafashi, S., Rasaei, M., Karimi, G., 2017. Effects of sugarcane and polyanionic cellulose on rheological properties of drilling mud: an experimental approach. Egyptian J. Petrol. 26, 371–374. https://doi.org/10.1016/j.ejpe.2016.05.009.

Kang, W., Mushi, S.J., Yang, H., Wang, P., Hou, X., 2020. Development of smart viscoelastic surfactants and its applications in fracturing fluid: a review. J. Pet. Sci. Eng. 190, 107107. https://doi.org/10.1016/j.petrol.2020.107107.

Karakosta, K., Mitropoulos, A.C., Kyzas, G.Z., 2021. A review in nanopolymers for drilling fluids applications. J. Mol. Struct. 1227, 129702. https://doi.org/10.1016/j.molstruc.2020.129702.

Katende, A., Boyou, N.V., Ismail, I., Chung, D.Z., Sagala, F., Hussein, N., Ismail, M.S., 2019. Improving the performance of oil based mud and water based mud in a high temperature hole using nanosilica nanoparticles. Colloids and surfaces A: physicochemical and engineering aspects 577, 645–673. https://doi.org/10.1016/j.colsurfa.2019.05.088.

Khamehchi, E., Shahin, T., Ali, A., 2016. Rheological properties of Aphron based drilling fluids. Petrol. Explor. Dev. 43 (6), 1076–1081. https://doi.org/10.1016/S1876-3804(16)30125-2.

Kök, M.V., Bal, B., 2019. Effects of silica nanoparticles on the performance of water-based drilling fluids. J. Pet. Sci. Eng. 180, 605–614. https://doi.org/10.1016/j.petrol.2019.05.069.

Kumar, S., Awang, M., Ahmed, S., Dehraj, N.U., Saleem, Y.S., 2015. Worm-Like Micelles as a mobility control agent for chemical enhanced oil recovery. In: SPE/IATMI Asia Pacific Oil & Gas Conference and Exhibition. OnePetro. https://

doi.org/10.2118/176075-MS.
Li, M.C., Ren, S., Zhang, X., Dong, L., Lei, T., Lee, S., Wu, Q., 2018a. Surface-chemistry-tuned cellulose nanocrystals in a bentonite suspension for water-based drilling fluids. ACS Appl. Nano Mater. 1, 7039–7051. https://doi.org/10.1021/acsanm.8b01830.
Li, M.C., Wu, Q., Song, K., French, A.D., Mei, C., Lei, T., 2018b. pH-responsive water-based drilling fluids containing bentonite and chitin nanocrystals. ACS Sustain. Chem. Eng. 6, 3783–3795. https://doi.org/10.1021/acssuschemeng.7b04156.
Li, M.C., Tang, Z., Liu, C., Huang, R., Koo, M.S., Zhou, G., Wu, Q., 2020a. Water-redispersible cellulose nanofiber and polyanionic cellulose hybrids for high-performance water-based drilling fluids. Ind. Eng. Chem. Res. 59 (32), 14352–14363. https://doi.org/10.1021/acs.iecr.0c02644.
Li, M.C., Wu, Q., Han, J., Mei, C., Lei, T., Lee, S.Y., Gwon, J., 2020b. Overcoming salt contamination of bentonite water-based drilling fluids with blended dual-functionalized cellulose nanocrystals. ACS Sustain. Chem. Eng. 8, 11569–11578. https://doi.org/10.1021/acssuschemeng.0c02774.
Li, X., Wang, K., Lu, Y., Shen, X., Zhang, H., Peng, J., Jiang, S., Duan, M., 2024. Compatibility and efficiency of hydrophilic/hydrophobic nano silica as rheological modifiers and fluid loss reducers in water-based drilling fluids. Geoene. Sci.Eng. 234, 212628. https://doi.org/10.1016/j.geoen.2023.212628.
Liu, H., Jin, X., Ding, B., 2016. Application of nanotechnology in petroleum exploration and development. Petrol. Explor. Dev. 43 (6), 1014–1021. https://doi.org/10.11698/PED.2016.06.20 (in Chinese).
Mahto, V., Sharma, V.P., 2004. Rheological study of a water based oil well drilling fluid. J. Pet. Sci. Eng. 45, 123–128. https://doi.org/10.1016/j.petrol.2004.03.008.
Mao, J., Yang, X., Chen, Y., Zhang, Z., Zhang, C., Yang, B., Zhao, J., 2018. Viscosity reduction mechanism in high temperature of a Gemini viscoelastic surfactant (VES) fracturing fluid and effect of counter-ion salt (KCl) on its heat resistance. J. Pet. Sci. Eng. 164, 189–195. https://doi.org/10.1016/j.petrol.2018.01.052.
Medhi, S., Chowdhury, S., Gupta, D.K., Mazumdar, A., 2020. An investigation on the effects of silica and copper oxide nanoparticles on rheological and fluid loss property of drilling fluids. J. Pet. Explor. Prod. Technol. 10, 91–101. https://doi.org/10.1007/s13202-019-0721-y.
Mohammadi, M., Mahani, H., 2020. Insights into the pore-scale mechanisms of formation damage induced by drilling fluid and its control by silica nanoparticles. Energy Fuel. 34, 6904–6919. https://doi.org/10.1021/acs.energyfuels.0c00605.
Nur, M.M., Saleh, T.A., 2022. Melamine-modified polyacrylic grafted on activated carbon and its efficiency for shale inhibition. Upstream Oil and Gas Technology 8, 100065. https://doi.org/10.1016/j.upstre.2022.100065.
Ogugbue, C.C., Rathan, M., Shah, S.N., 2010. Experimental investigation of biopolymer and surfactant based fluid blends as reservoir drill-in fluids. SPE Oil and Gas India Conference and Exhibition, Mumbai, India. https://doi.org/10.2118/128839-MS.
Olatunde, A.O., Usman, M.A., Olafadehan, O.A., Adeosun, T.A., Ufot, O.E., 2012. Improvement of rheological properties of drilling fluid using locally based materials. Petroleum & Coal 54 (1), 65–75.
Olmos, C.M., Vaca, A., Rosero, G., Peñaherrera, A., Perez, C., de Sá Carneiro, I., Vizuete, K., Arroyo, C.R., Debut, A., Pérez, M.S., Cumbal, L., Lerner, B., 2019. Epoxy resin mold and PDMS microfluidic devices through photopolymer flexographic printing plate. Sensor Actuat B: Chem 288, 742–748. https://doi.org/10.1016/j.snb.2019.03.062.
Oseh, J.O., Norddin, M.N.A.M., Duru, U.I., Ismail, I., Ngouangna, E.N., Yahya, M.N., Gbadamosi, A.O., Agi, A., Odo, J.E., Ofowena, F.O., Ndagi, U.B., 2024. Comparison of water-based drilling muds with hydroxyapatite nanoparticles and copper II oxide nanoparticles for lifting cuttings through rotating drill pipes at different hole inclinations. Arabian J. Sci. Eng. 49, 8997–9025. https://doi.org/10.1007/s13369-024-09007-4.
Oseh, J.O., Norddin, M.N.A.M., Ismail, I., Duru, U.I., Gbadamosi, A.O., Agi, A., Ngouangna, E.N., Blkoor, S.O., Yahya, M.N., Risal, A.R., 2023. Rheological and filtration control performance of water-based drilling muds at different temperatures and salt contaminants using surfactant-assisted novel nano-hydroxyapatite. Geoene. Sci.Eng. 228, 211994. https://doi.org/10.1016/j.geoen.2023.211994.
Philippova, O.E., Molchanov, V.S., 2019. Enhanced rheological properties and performance of viscoelastic surfactant fluids with embedded nanoparticles. Curr. Opin. Colloid Interface Sci. 43, 52–62. https://doi.org/10.1016/j.cocis.2019.02.009.
Rafati, R., Smith, S.R., Sharifi Haddad, A., Novara, R., Hamidi, H., 2018. Effect of nanoparticles on the modifications of drilling fluids properties: a review of recent advances. J. Pet. Sci. Eng. 161, 61–76. https://doi.org/10.1016/j.petrol.2017.11.067.
Rana, A., Khan, I., Ali, S., Saleh, T.A., Khan, S.A., 2020. Controlling shale swelling and fluid loss properties of water-based drilling Mud via ultrasonic impregnated SWCNTs/PVP nanocomposites. Energy Fuel. 34, 9515–9523. https://doi.org/10.1021/acs.energyfuels.0c01718.
Saleh, T.A., 2018. Nanotechnology in Oil and Gas Industries. Springer, Cham, Switzerland, p. 75.
Saleh, T.A., 2022a. Advanced trends of shale inhibitors for enhanced properties of water-based drilling fluid. Upstream Oil and Gas Technology 8, 100069. https://doi.org/10.1016/j.upstre.2022.100069.
Saleh, T.A., 2022b. Experimental and analytical methods for testing inhibitors and fluids in water-based drilling environments. TrAC, Trends Anal. Chem. 149, 116543. https://doi.org/10.1016/j.trac.2022.116543.
Saleh, T.A., Rana, A., Arfaj, M.K., Ibrahim, M.A., 2022. Hydrophobic polymer-modified nanosilica as effective shale inhibitor for water-based drilling mud. J. Pet. Sci. Eng. 209, 109868. https://doi.org/10.1016/j.petrol.2021.109868.
Salih, A.H., Elshehabi, T.A., Bilgesu, H.I., 2016. Impact of nanomaterials on the rheological and filtration properties of water-based drilling fluids. SPE Eastern Regional Meeting, Canton, Ohio, USA. https://doi.org/10.2118/184067-MS.
Smith, S.R., Rafati, R., Sharifi Haddad, A., Cooper, A., Hamidi, H., 2018. Application of aluminium oxide nanoparticles to enhance rheological and filtration properties of water based muds at HPHT conditions. Colloids Surf. A Physicochem. Eng. Asp. 537, 361–371. https://doi.org/10.1016/j.colsurfa.2017.10.050.
Sui, Z.M., Chen, X., Wang, L.Y., Xu, L.M., Zhuang, W.C., Chai, Y.C., Yang, C.J., 2006. Capping effect of CTAB on positively charged Ag nanoparticles. Physica E Low Dimens Syst Nanostruct 33, 308–314. https://doi.org/10.1016/j.physe.2006.03.151.
Tahr, Z., Ali, J.A., Mohammed, A.S., 2023. Sustainable aspects behind nano-biodegradable drilling fluids: a critical review. Geoene. Sci.Eng. 222, 211443. https://doi.org/10.1016/j.geoen.2023.211443.
Tahr, Z., Mohammed, A., Ali, J.A., 2022. Surrogate models to predict initial shear stress of clay bentonite drilling fluids incorporated with polymer under various temperature conditions. Arabian J. Geosci. 15, 1449. https://doi.org/10.1007/s12517-022-10720-3.
Trivedi, M.K., Dahryn Trivedi, A.B., 2015. Spectroscopic characterization of disodium hydrogen orthophosphate and sodium nitrate after biofield treatment. J. Chromatogr. Separ. Tech. 6 (5), 100282. https://doi.org/10.4172/2157-7064.1000282.
Villada, Y., Busatto, C., Casis, N., Estenoz, D., 2022. Use of synthetic calcium carbonate particles as an additive in water-based drilling fluids. Colloids Surf. A Physicochem. Eng. Asp. 652, 129801. https://doi.org/10.1016/j.colsurfa.2022.129801.
Villada, Y., Iglesias, M.C., Casis, N., Erdmann, E., Peresin, M.S., Estenoz, D., 2018. Cellulose nanofibrils as a replacement for xanthan gum (XGD) in water based muds (WBMs) to be used in shale formations. Cellulose 25, 7091–7112. https://doi.org/10.1007/s10570-018-2081-z.
Villada, Y., Iglesias, M.C., Olivares, M.L., Casis, N., Zhu, J., Peresin, M.S., Estenoz, D., 2021. Di-carboxylic acid cellulose nanofibril (DCA-CNF) as an additive in water-based drilling fluids (WBMs) applied to shale formations. Cellulose 28, 417–436. https://doi.org/10.1007/s10570-020-03502-1.
Wang, J., Feng, Y., Agrawal, N.R., Raghavan, S.R., 2017. Wormlike micelles versus water-soluble polymers as rheology-modifiers: similarities and differences. Phys. Chem. Chem. Phys. 19, 24458–24466. https://doi.org/10.1039/c7cp04962e.
Yang, Y., Zhang, H., Wang, H., Zhang, J., Guo, Y., Wei, B., Wen, Y., 2022. Pseudo-interpenetrating network viscoelastic surfactant fracturing fluid formed by surface-modified cellulose nanofibril and wormlike micelles. J. Pet. Sci. Eng. 208, 109608. https://doi.org/10.1016/j.petrol.2021.109608.
Yayapao, O., Thongtem, T., Phuruangrat, A., Thongtem, S., 2011. CTAB-assisted hydrothermal synthesis of tungsten oxide microflowers. J. Alloys Compd. 509, 2294–2299. https://doi.org/10.1016/j.jallcom.2010.10.204.